UKACC International Conference on Control 2012
Cardiff, UK, 3-5 September 2012

# Experimental Verification of Best Linear Approximation of a Wiener System for Binary Excitations

Hin Kwan Wong
School of Engineering
University of Warwick
Coventry, UK CV4 7AL
Email: Hin.Wong@warwick.ac.uk
Telephone: (44) 2476 572904

Johan Schoukens
ELEC Dept.
Vrije Universiteit Brussel
1050 Brussels, Belgium
Email: Johan.Schoukens@vub.ac.be
Telephone: (32) 2629 2944

Keith Godfrey
School of Engineering
University of Warwick
Coventry, UK CV4 7AL
Email: K.Godfrey@warwick.ac.uk
Telephone: (44) 2476 523144

***Abstract*—The Best Linear Approximation (BLA) is a linearisation of the transfer characteristics of a nonlinear system in a least squares sense. The BLA is known to depend on the statistical properties of the input signal used to identify it. The theory for Gaussian input sequences has been known for several years, but the corresponding theory for binary input sequences has only recently been developed. In this paper, experiments on a physical electronic Wiener system, aimed at verification of predictions made for the differences between BLA's estimated using Gaussian sequences and those estimated using binary sequences, are described. The results were found to be a good match with the theory but difficulties encountered during the experiment highlight a need for further work in extending the discrete-time theory to the continuous-time domain.**

## I. Introduction

In system identification, the frequency response function or the impulse response of a system contains information about the system. Based on this information, one can model, make prediction and control the system to produce desired behaviour. All systems are nonlinear to some extent, and in some systems the nonlinearity plays a significant role. Even so, linearising a nonlinear system has merits in modelling and control, and the Best Linear Approximation (BLA) [1–5], which is a linear model minimising the expected value of mean squared difference between the actual output of the system and the modelled output is particularly useful for this. The BLA however, depends on the power and amplitude distribution of the excitation signals used to identify it [6]. This paper verifies the theory developed by Wong et al. [6] for binary input signals through experiments on a physical electronic system with a linear low-pass filter and a cubic nonlinearity in a Wiener configuration.

## II. Experiment Setup

The system was set up using the equipment listed below, and following the system schematic shown in Figure 1. The HP VXI mainframe was connected to a desktop computer with the MATLAB software. Data analysis was performed through MATLAB.

### A. List of equipment

- HP E1401B VXI mainframe with:
  - VXI-MXI-2 interface card
  - $2\times$ HP E1430A $10\,\text{MSa/s}$ 23-bit ADCs, with filtering and memory (henceforth referred to as 'acquisition card')
  - HP E1445A arbitrary function generator card
- Desktop computer with PCI-MXI-2 interface card
- Non-inverting pre-buffer with AD8610A op-amp
- Non-inverting post-buffer with TL071CP op-amp
- $2\times 50\,\Omega$ matched impedance buffers
- RC filter circuit with changeable resistors and capacitors
- $50\,\Omega$ matched impedance measurement buffers
- Pre-built cubic nonlinearity circuit
  - based on AD532JH four-quadrant multipliers
- Tektronix TDS 2001C Oscilloscope
- $\pm 12\,\text{V}$ and $\pm 15\,\text{V}$ power supplies
- A $1.5\,\text{nF}$ capacitor with either $2.7\,\text{k}\Omega$, $27\,\text{k}\Omega$ or $110\,\text{k}\Omega$ resistors in the RC filter,
  - giving cut-off frequency values of $f_{\text{co}} = 39.3\,\text{kHz}$, $3.93\,\text{kHz}$ and $0.965\,\text{kHz}$ respectively.

### B. Methodology

The objective is to verify theoretical difference between the BLA's obtained from the use of Maximum Length Binary Sequences (m-sequences) [7], and from Gaussian signals, more specifically random phase multisines [2]. The linearity was a simple RC filter circuit, and the nonlinearity was a static cubic power function. Three sets of experiments were performed, each with a different combination of time constants for the linearity. The resistor values used were $2.7\,\text{k}\Omega$, $27\,\text{k}\Omega$ and $110\,\text{k}\Omega$. The capacitor value was fixed at $1.5\,\text{nF}$, for a reason which will be explained in Section II-D.

Table I lists parameters and their values used in the experimental work. Both types of input were subjected to supersampling (see Section II-D). However, the bandwidth of the multisine was set equal to the clock frequency of the binary

978-1-4673-1558-6/12/$31.00 ©2012 IEEE

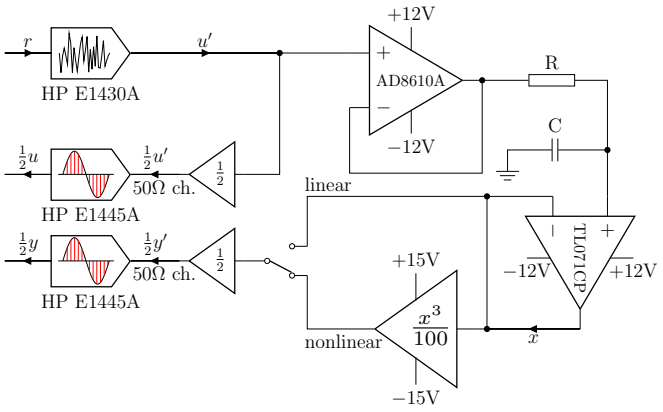


Figure 1. System schematic

sequence. This was performed so that after downsampling (also see Section II-D) at the measurement, both types of signal will have identical bandwidth and the spectral 'whiteness' of the two signal types could be preserved. The whiteness of the input spectrum constitutes one of the assumptions of the original discrete time BLA theory in Wong et al. [6].

The general procedure of data collection of the experiment for both the linear and nonlinear cases was as follows:

1) Generate the reference signal $r$, either:
   a) a discrete random-phase multisine for the Gaussian case, or:
   b) a Maximum Length Binary Sequence of period $N_{\text{base}} = 511$ samples for the binary case.
2) Realise the periodic signal using the HP E1445A arbitrary function generator card. The excitation is uninterrupted and continuously turned on from this point onwards.
3) Pause for 5 seconds so that transient effects in the measurements are expected to be negligible.
4) Initiate measurements with the acquisition cards and collect $P$ periods of data. The measurement intervals are internally synchronised with the generator.
5) Due to internal attenuation of the matched impedance buffers, measurements are normalised by a factor of two to obtain $u$ and $y$ (in multiple periods).
6) Go to Step 1 and repeat for a different realisation of input until $M$ data sets of different input realisations are obtained.

Note that across the $M$ sub-experiments, the same input sequence realisation was never used twice.

### C. Robust non-parametric identification procedure

Given a set of input and output data from $M$ sub-experiments of independent input realisations, each with $P$ periods of steady-state measurements, robust estimator for the BLA is given as:

$$\hat{G}_{\text{BLA}}(\mathrm{j}\omega) = \frac{\sum_{m=1}^{M}\sum_{p=1}^{P} Y_{[m,p]}U^{\star}_{[m,p]}}{\sum_{m=1}^{M}\sum_{p=1}^{P} U_{[m,p]}U^{\star}_{[m,p]}} \tag{1}$$

where $U_{[m,p]}$ and $Y_{[m,p]}$ contain the $m^{\text{th}}$ sub-experiment and $p^{\text{th}}$ period of the measured input spectrum $U(\mathrm{j}\omega)$ and the measured output spectrum $Y(\mathrm{j}\omega)$. The $^{\star}$ symbol denotes complex conjugate. For reasons stated in II-D, the measured input spectrum for the binary excitation case, $U_{[m,p]}$ is taken as the reference input spectrum $R_{[m]}(\mathrm{j}\omega)$.

The estimator is robust against noise disturbances and is unbiased if input noise levels are small.

### D. Supersampling

The HP VXI system is capable of any sampling frequency up to and including 10 MHz. In the experiment, the measurements were oversampled by a factor of $\mu$ above the frequency of the binary sequence input $f_{\text{c}}$. The upper frequency of the bandwidth of the random phase multisine $f_{\text{w}}$ was set equal to $f_{\text{c}}$. The measurement data were then subjected to manual downsampling by the same factor $\mu$. This results in both input signal types having identical bandwidth. The supersampling and the subsequent downsampling were performed for two main reasons detailed in the next two subsections (Ringing and Overshoot; Anti-alias).

The RC filter has low-pass (smoothing) characteristics. To downsample (or subsample) the measurement, a location of the highest peak (or lowest trough) of the output signal was taken as the reference point. From this reference point onwards and backwards every $\mu^{\text{th}}$ sample was taken as an idealised zero-order-hold (ZOH) measurement, with the ZOH clock frequency a factor $\mu$ lower than the original sampling (hence a downsampling). The reference signal $r$ and the measured output $y$ were also aligned through this reference point, so that the peaks of the output after RC filtering would then occur directly after the switching points of the binary reference input. The procedure is more easily appreciated by referring to Figure 2 by comparing the reference input (dotted line) and the two red solid lines representing the original high frequency sampling and the subsequent downsampled and aligned ZOH data. If there were no ringing, overshoot, nonlinear effects or noise, this subsampling procedure would result in a perfect reconstruction of the behaviour of an ideal ZOH sampler according to discrete-time theory. This had been verified by simulation. This subsampling procedure is performed for both linear and nonlinear measurements. Since this procedure can only be reliably performed through the easily visible binary switching points, the same alignment amount and reference point time coordinate were used for the corresponding case with multisine input.

*Ringing and overshoot:* During testing with binary excitation signals, it was observed through the oscilloscope that

Table I
TABLE OF PARAMETERS AND SETTINGS

| Symbol | Description | Value (units) |
|---|---|---|
| $f_s$ | Sampling frequency for the arbitrary waveform generator, and acquisition cards. The Nyquist frequency is then $f_s/2$. | 312.5 kHz |
| $T_s$ | Sampling interval $= 1/f_s$. | 3.2 µs |
| $\mu$ | Over-sampling ratio for m-sequences (see Section II-D). | 8 |
| $f_c$ | Clock frequency of the m-sequences $(= f_s/\mu)$. | 39⅛ kHz |
| $T_b$ | Bit interval for the m-sequences $(= 1/f_c)$. | 25.6 µs |
| $f_w$ | Bandwidth of the multisine sequence before downsampling $(= f_c = f_s/\mu)$. | 39⅛ kHz |
| $f_{aa}$ | Anti-aliasing filter cut-off frequency $\equiv 0.4 f_s$. This coupling with the sampling frequency value is internally enforced by the HP1430A acquisition cards. | 125 kHz |
| $N_{base}$ | Base length of sequence after subsampling, (= length of a 9-tap m-sequence) | 511 Sa† |
| $N$ | Length of a data record $(= \mu N_{base})$. | 4088 Sa† |
| $P$ | Number of periods measured (linear case; nonlinear case). | 12; 4 |
| $M$ | Number of independent realisations (linear case; nonlinear case). | 5; 16 |
| $V_{rms}$ | RMS voltage of the input signals. | 1.5 V |

†Sa = samples

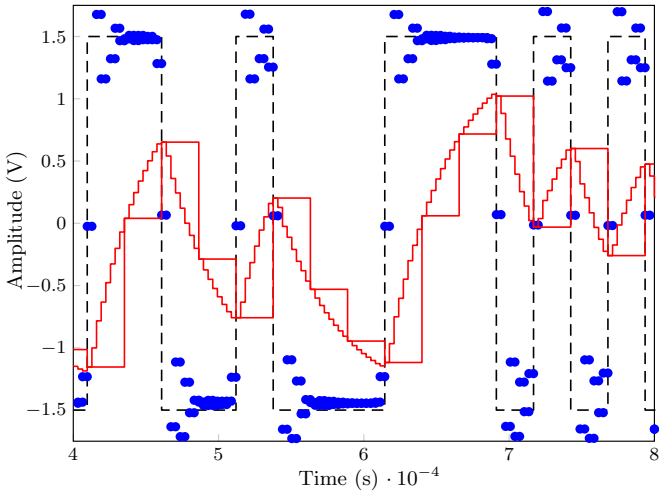


Figure 2. The use of supersampling and subsampling – Reference input (black dotted line), Measured input (blue dots), Measured output: a) supersampled and b) subsampled (red solid lines).

all operational amplifier (op-amp) based electronic buffers introduce high frequency oscillations in form of ringing to a varying extent. This is caused by non-ideal step-response characteristics when load or parasitic capacitances at output of op-amps introduce unintended poles in the transfer characteristics of the op-amps through feedback. The datasheets of many op-amps have step-response graphs which illustrate this.

In this experiment setup, the overshoots and undershoots were especially large, up to 20% with the pre-buffer due to the capacitive load at the RC circuit, even when a higher quality op-amp (with regards to its ability in driving capacitive loads) was used [8]. The overshoot depends on the load or parasitic capacitance hence the load capacitor $C$ of the RC circuit was fixed at 1.5nF for consistency.

Moreover, the HP E1430A acquisition cards themselves have significant overshoots that can be seen in the measurement data, although the oscilloscope suggested the actual acquisition inputs $u'$ and $y'$ were relatively free of such effects. This may be caused by the high order high cut-off frequency anti-aliasing filter having oscillatory step responses. The ringing at the measured input channel from an acquisition card can be seen in Figure 2. This phenomenon persisted with an Agilent 33120A waveform generator directly driving the acquisition cards, isolated completely from the system in question.

While the RC passively forms a low pass filter and is capable of minimising the effect of ringing from the pre-buffer, overshoot and ringing from the acquisition cards are inevitable. Due to the nature of sample-and-hold at the acquisition cards, the use of supersampling is necessary to obtain measurements of acceptable accuracy. The BLA theory developed is incapable of modelling in continuous time domain of such effects at the moment.

For multisine input sequences, there are no noticeable ringing or overshoot effects.

Because of the overshoot and ringing present in the measurement data from the HP E1430A acquisition cards, the signal sequence $u$ is no longer reliable and accurate representation of $u'$ in the m-sequence case. Henceforth in dealing with binary sequences, the reference signal $r$ is used as the basis for identification.

In addition, manual alignment of the measured input and output signals can be performed.

*Anti-alias:* It is necessary to minimise the effect of anti-aliasing filters on the measurements because of the use of the ideal reference signal $r$ instead of measured input $u$ in the case of binary excitations. In addition, the nonlinearity broadens the bandwidth of the output, which then may be interfered with by the anti-aliasing filter if action is not taken. Supersampling allows the internal anti-aliasing filter to be bypassed since the internal anti-aliasing filter of the HP E1430A acquisition cards have their cut-off frequencies $f_{\text{aa}}$ dependent upon the sampling frequency $f_{\text{s}}$ (see Table I). The combination of the specified low bandwidth of the multisine, the discrete nature of binary excitation signals and the low pass characteristics of RC mean that any real aliasing effect was negligible. It has been shown that broadening of spectrum due to nonlinearity would result in aliased components that are never coherent with the original input component [2, Theorem 3.21], hence the lack of anti-aliasing filter would only act as additional uncorrelated noise in the BLA measurement.

### E. Linear measurements

Measurements were performed to identify either a parametric or a non-parametric model for the linearity. The rms signal amplitudes for the Gaussian and binary signals were both set to 1.5 V. The non-parametric model was obtained using (1), and a parametric model was fitted where suitable using the iterative weighted nonlinear least squares procedure provided by ELiS in the *fdident* toolbox for MATLAB [9]. The weighting factors were proportional to the reciprocal of the variances at each frequency point. The isolation provided by the pre-buffer and post-buffer for the RC circuit introduced some additional linear dynamics, and hence suitable single pole models could not be fitted to the data. When a parametric model of order four is not sufficient to describe the transfer characteristics of the linearity in both the z-domain and the s-domain, the non-parametric model is used. This was the case for when the resistor value was 110 kΩ, and hence Figure 6 does not contain the results from the parametric model.

Figure 3 shows an example of the result of a non-parametric linearity identification. The noise variances indicate levels of exogenous additive noise from the environment whereas the total variances indicate the levels of nonlinear distortions plus environment noise. There is a discrepancy between the result obtained with multisine sequences and that obtained from m-sequences. This suggests input dependent nonlinear characteristics which include some effect from ringing oscillations.

As an example, for $R = 27\,\text{k}\Omega$ and with $C = 1.5\,\text{nF}$, the time constant $T_{\text{p}} = 27{\times}10^{3} \cdot 1.5{\times}10^{-9} = 4.05{\times}10^{-5}$ seconds. With a sampling interval $T_{\text{c}}$ given by $1/f_{\text{c}} = (39^{1}/_{16} \times 10^{3})^{-1}$ seconds, $T_{\text{c}}/T_{\text{p}} = 0.6321$, and therefore the theoretical transfer function is:

$$G(\text{z}) = \frac{\text{z}}{\text{z} - e^{-0.6321}} = \frac{\text{z}}{\text{z} - 0.5315}. \qquad (2)$$

The parametric model identified for the m-sequence case with sampling time $T_{\text{c}}$ was:

$$\hat{G}(\text{z}) = \frac{0.01011(\text{z} + 41.23)(\text{z} + 0.05967)}{(\text{z} - 0.5481)(\text{z} + 0.01818)}. \qquad (3)$$

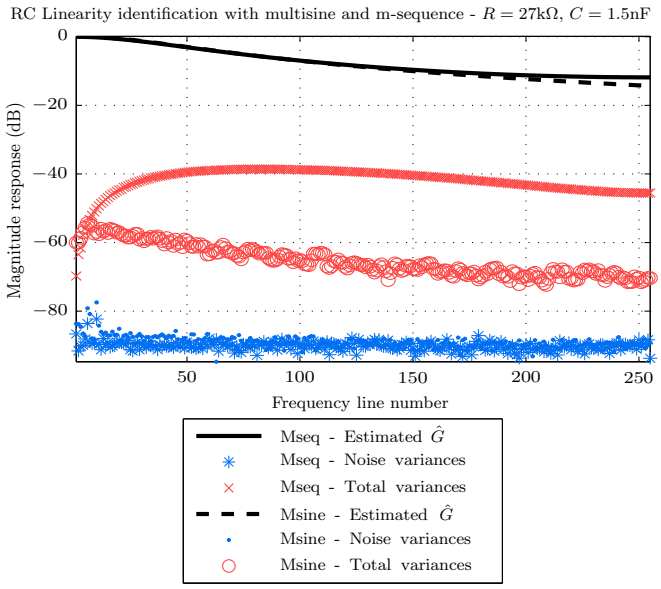


Figure 3. RC Linearity identification with op-amp based pre- and post-buffers. (To convert to frequency (Hz), line number should be multiplied by $f_{\text{s}}/(8 \times 511)$)

It can be seen that the estimated positive pole is very close to the theoretical value, but as noted above, the pre-buffer and the post-buffer to the RC circuit introduced some additional dynamics, with a negative zero and a negative pole very close to the origin, and a further negative zero that is so large that it can be regarded as a constant over the frequency range of interest.

Despite the fact that the system under test was linear, there were nonlinear distortions in both input cases and the level was higher for the binary input. This was due to to be nonlinear effects from the unity-gain op-amp buffers, especially from the pre-buffer which had to drive the capacitive load. Ringing oscillations were especially noticeable with binary inputs (see II-D). If the buffers were not used, the nonlinear distortions disappear regardless of the input signal. However, due to current driving limitation of the signal generator and the capacitive load, there was unacceptable distortion of the realised input for the binary case, hence the buffers were necessary.

### F. Nonlinear measurements and BLA theory

The nonlinear measurements were obtained in a similar manner to the linear measurement case. The non-parametric BLA was obtained using (1).

To enable comparison with the theory, additional information is required. This includes the even higher order moments of the input signals, the signal power (or the rms value $V_{\text{rms}}$), the impulse response of the linearity and the polynomial coefficients of the nonlinearity. For the Gaussian case, the even order moments of $u$ (i.e., $\text{E}[u^n]$) were measured and averaged for a single experiment, for even $n$. For the binary case, $u$ was replaced by $r$ hence $\text{E}[r^n] = V_{\text{rms}}^n$. The impulse response of the linearity was taken from the parametric model

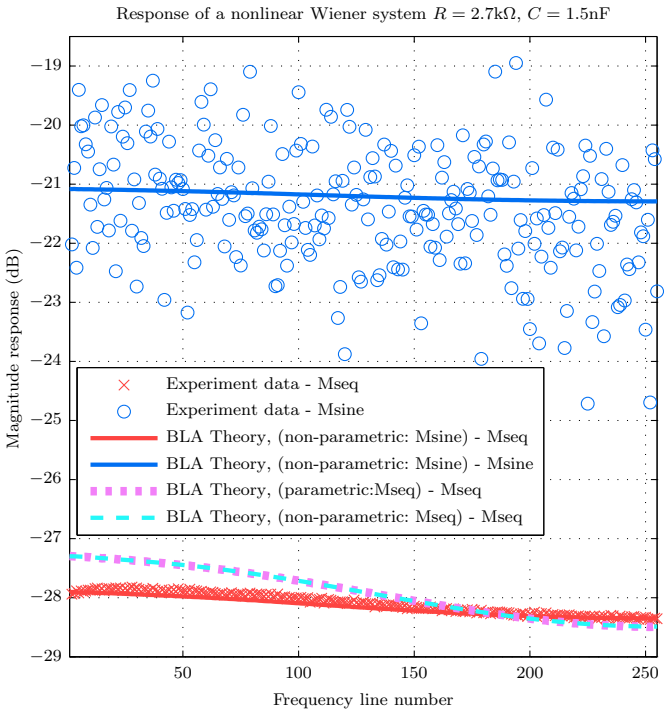


Figure 4. Experiment result of the identification of the BLA with Gaussian and binary inputs for an electronic Wiener system with non-ideal cubic nonlinearity and a RC linearity with $R = 2.7\text{k}\Omega$, $C = 1.5\text{nF}$ giving corner frequency $f_{\text{co}} = 39.3\text{kHz}$. (For conversion from frequency line number to Hz, see caption of Figure 3.)

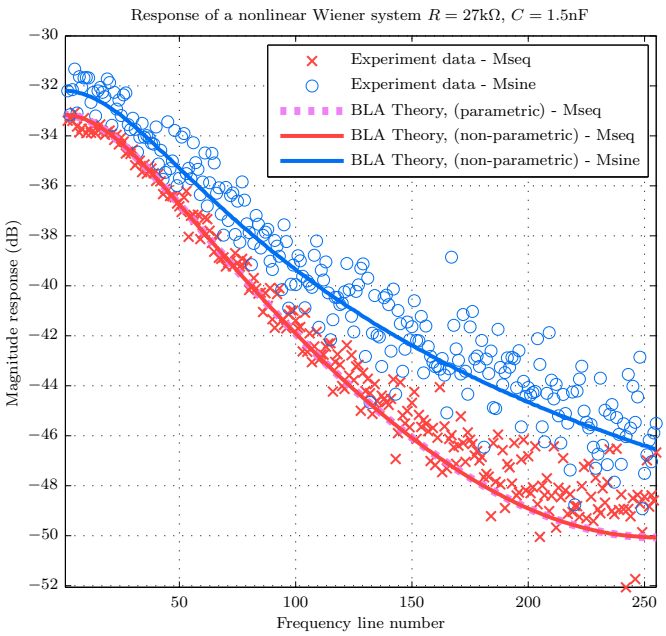


Figure 5. As Figure 4, but with $R = 27\text{k}\Omega$, giving corner frequency $f_{\text{co}} = 3.93\text{kHz}$.

if available, and the non-parametric model by inverse Fourier transform. Finally, the nonlinearity was identified by simple least squares polynomial regression performed on 20 periods of output data obtained from the nonlinearity with a multisine excitation as a direct input to the nonlinearity. The polynomial fitted to the nonlinearity was:

$$\begin{aligned} \text{f}_{\text{NL}}(x) = 0.01088x^3 - 0.001356x^2 \\ +0.008169x + 0.05816. \end{aligned} \tag{4}$$

The cubic electronic circuit had a transfer characteristic of $\text{f}_{\text{NL}}(x) = 0.01x^3$ as shown in Figure 1. Due to non-ideal characteristics there was a non-negligible quadratic term together with a linear term and a dc component in the fitted characteristic. Neither the quadratic term nor the dc offset enter into the theoretical calculations, but the linear component does, and it was taken into account in the comparisons between theory and the practical results described in Section III.

## III. Results and Analysis

Figure 4, 5 and 6 show the comparison of the BLA obtained through experiment results and those obtained from theory, for a Wiener system with (non-ideal, see (4)) cubic nonlinearity and RC filter linearity with $C = 1.5\text{nF}$ for all three cases and $R = 2.7\,\text{k}\Omega$, $27\,\text{k}\Omega$ and $110\,\text{k}\Omega$ respectively.

With $R = 2.7\,\text{k}\Omega$, the RC filter has a cut-off (or corner) frequency of $f_{\text{co}} = 1/2\pi RC \approx 39.3\,\text{kHz}$ and acts as an all-pass filter since the binary signal clock frequency was $f_{\text{c}} = 39\text{1}/\text{16}\,\text{kHz}$. Unfortunately this means ringing and overshoot effects (see Section II-D) were significant immediately after the RC filter stage. The linearity identification using m-sequences would yield unreliable results despite subsampling techniques. Here the use of non-parametric models of the linearity identified by a multisine was more suitable for the BLA theory. This can be seen by the fact that in Figure 4 the solid red line, representing the BLA theory based on a non-parametric linearity model identified with a multisine sequence, was able to match the experiment data represented by crosses more closely than that based on a linearity model (parametric or non-parametric) identified with a m-sequence. There are minimal differences between results derived from the non-parametric and parametric linearity models—the plots (cyan dashed and magenta heavy-dotted, respectively) are very close to each other.

For $R = 27\,\text{k}\Omega$, the RC filter had a corner frequency of approximately $3.93\,\text{kHz}$. Ringing and overshoot effects were then negligible immediately after the RC filter stage. Here the non-parametric models of the linearity for the m-sequence and multisine were used for their respective counterparts. In addition, the parametric model of (3) from Section II-E was used in the BLA theory to calculate the biased theoretical BLA for binary sequences. There were no discernible differences in the BLA theory calculated from the non-parametric and parametric linearity models as shown by the overlapping of the heavy-dotted magenta line and the solid red line in Figure 5.

When $R = 110\,\text{k}\Omega$, the RC filter had a corner frequency of about $0.965\,\text{kHz}$. The result is illustrated in Figure 6. This time parametric models up to order four produced by ELiS could not produce adequate quality fit to the transfer function of the linearity. Nevertheless the BLA theory based on the

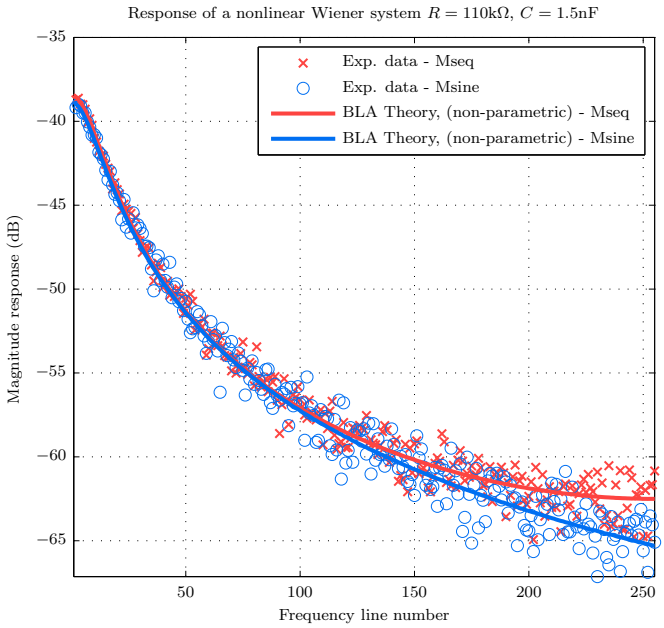


Figure 6. As Figure 4, but with $R = 110\text{k}\Omega$, giving corner frequency $f_{\text{co}} = 0.965\,\text{kHz}$.

non-parametric models was able to match the experiment data in both the gain and the shape of the transfer characteristics.

As the time constant of the system increases, the length of the impulse response of the system increases. It has been shown in Wong et al. [6] that this results in a BLA estimated by a signal with an arbitrary amplitude distribution converging to that obtained from Gaussian signal. This is also observed in Figures 4 to 6.

## IV. Conclusions

For all three sets of experiments investigated, it can be seen that the BLA theory prediction and experiment result are in good agreement. This is despite the fact that the BLA theory was based on impulse responses of the linearity modelled as finite-impulse-response (FIR) filters, whereas here the RC filter circuit is an infinite-impulse-response (IIR) filter.

The difficulties encountered with the experiment, mainly the ringing and overshoot effects illustrate a weakness in the z-domain discrete-time theory. It may therefore be beneficial to extend the theory to the continuous-time s-domain.

## Acknowledgement

H. K. Wong was supported by a Doctoral Training Grant from the U.K. Engineering and Physical Sciences Research Council (EPSRC). The work was supported in part by the Fund for Scientific Research (FWO-Vlaanderen), by the Flemish Government (Methusalem), and by the Belgian Government through the Inter-University Poles of Attraction (IUAP VI/4) Program.

## References

[1] M. Enqvist and L. Ljung, 'Linear approximations of nonlinear FIR systems for separable input processes', Department of Electrical Engineering, Linköping University, SE-581 83 Linköping, Sweden, Tech. Rep. LiTH-ISY-R-2718, Dec. 2005.

[2] R. Pintelon and J. Schoukens, *System identification: a frequency domain approach*, 2nd ed. Hoboken, NJ: Wiley-IEEE Press, 2012.

[3] P. M. Mäkilä and J. R. Partington, 'Least-squares LTI approximation of nonlinear systems and quasistationarity analysis', *Automatica*, vol. 40, pp. 1157–1169, Jul. 2004.

[4] P. M. Mäkilä, 'On optimal LTI approximation of nonlinear systems', *IEEE Trans. Autom. Control*, vol. 49, no. 7, pp. 1178–1182, Jul. 2004.

[5] ——, 'LTI approximation of nonlinear systems via signal distribution theory', *Automatica*, vol. 42, pp. 917–928, Jun. 2006.

[6] H. K. Wong, J. Schoukens and K. R. Godfrey, 'Analysis of best linear approximation of a Wiener-Hammerstein system for arbitrary amplitude distributions', *IEEE Trans. Instrum. Meas.*, vol. 61, no. 3, pp. 645–654, Mar. 2012.

[7] K. R. Godfrey, 'Introduction to perturbation signals for time-domain system identification', in *Perturbation Signals for System Identification*, K. R. Godfrey, Ed., Hemel Hempstead: Prentice-Hall, 1993, ch. 1.

[8] *AD8610A datasheet*, One Technology Way, P.O. Box 9106, Norwood, MA 02062-9106, U.S.A.: Analog Devices.

[9] I. Kollár, *Frequency Domain System Identification Toolbox for use with MATLAB*. Natick, MA: MathWorks Inc., 1994.